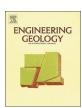
ELSEVIER

Contents lists available at ScienceDirect

Engineering Geology

journal homepage: www.elsevier.com/locate/enggeo



Stability of 3D slope under steady unsaturated flow condition



Z.W. Li*, X.L. Yang

School of Civil Engineering, Central South University, Changsha, Hunan 410075, China

ARTICLE INFO

List of symbols

Keywords: Slope stability Steady unsaturated flow condition 3D failure mechanism Stability number

ABSTRACT

Slope stability has commonly been analyzed by considering dry or saturated soils under two-dimensional (2D) plane-strain conditions. However, in practice, soils are often unsaturated, and many slope failures exhibit a three-dimensional (3D) feature. In this study, the kinematic limit analysis method is adopted to estimate the stability of slopes subjected to vertical unsaturated steady flow in the context of a 3D rotational failure mechanism. A closed-form representation is employed to express the shear strength behavior of unsaturated soils. According to the work-energy balance equation, the critical cohesion for a slope in the limit state is calculated and listed in the form of a stability number. An optimization scheme is used to search for the maximum stability number. By comparing with the previously published 2D and 3D solutions, the proposed method is validated. Charts of different parameters are plotted for parametric analysis and practical use in the design of slopes. It is shown that accounting for the 3D effect and the soil suction can lead to a less conservative result. This paper provides a useful method for assessing the combined effect of 3D boundary conditions and unsaturated flow conditions on the stability of slope and gives some useful suggestions for engineering application.

Pore size distribution parameter

S	n	Pore size distribution parameter
	$N_{ m s}$	Stability number
	ω	Angular velocity of failure mechanism
Parameters shown in Fig. 1	q	Vertical specific discharge
Inverse of air entry pressure	R	Circle radius
Slope width	r, r'	Distances from rotation center to generic points on
Ratio of width to height of slope		curves AC and A´C´
Width of inserted block	$r_{0}, r_{0}^{'}$	Initial distances from rotation center to curves AC
Maximum width of 3D portion	0, 0	and A´C´
Slope inclined angle	$r_{0}^{'}/r_{0}$	Ratio of r_0 to r_0
Effective cohesion and internal friction angle of soil	S_{t}	Sliding surface
Apparent cohesion caused by suction stress	$\sigma^{'}$	Effective stress
Apparent cohesion along sliding surface for 3D	σ	Total stress
portion and inserted portion	σ^{s}	Suction stress
Internal energy dissipation rate caused by soil	$\sigma - u_a$	Net stress on failure plane
cohesion	θ	Rotation angle of failure mechanism
Internal energy dissipation rate caused by apparent	$\theta_0, \theta_{ m h}$	Minimum and maximum rotation angle of failure
cohesion		mechanism
Internal energy dissipation rate due to apparent	$ heta_{ m B}$	Rotation angle between horizontal line and line
cohesion for 3D portion and inserted portion		segment OB
Slope height	$ au_{ m f}$	Shear strength of unsaturated soil
Unit weight of soil	u_a	Pore air pressure
Unit weight of water	$u_a - u_w$	Matric suction
Saturated hydraulic conductivity	u_w	Pore water pressure
Length of line segment AB in Fig. 1	ν	Velocity of a generic point on sliding surface
	Parameters shown in Fig. 1 Inverse of air entry pressure Slope width Ratio of width to height of slope Width of inserted block Maximum width of 3D portion Slope inclined angle Effective cohesion and internal friction angle of soil Apparent cohesion caused by suction stress Apparent cohesion along sliding surface for 3D portion and inserted portion Internal energy dissipation rate caused by soil cohesion Internal energy dissipation rate caused by apparent cohesion Internal energy dissipation rate due to apparent cohesion for 3D portion and inserted portion Slope height Unit weight of soil Unit weight of water Saturated hydraulic conductivity	Parameters shown in Fig. 1 Inverse of air entry pressure Slope width Ratio of width to height of slope Width of inserted block Maximum width of 3D portion Slope inclined angle Effective cohesion and internal friction angle of soil Apparent cohesion caused by suction stress Apparent cohesion along sliding surface for 3D portion and inserted portion Internal energy dissipation rate caused by soil cohesion Internal energy dissipation rate caused by apparent cohesion Internal energy dissipation rate due to apparent cohesion for 3D portion and inserted portion Slope height Unit weight of soil Unit weight of water Saturated hydraulic conductivity Length of line accompant AB in Fig. 1

^{*} Corresponding author.

E-mail addresses: lizhengw@163.com (Z.W. Li), yangxl@csu.edu.cn (X.L. Yang).

Z.W. Li, X.L. Yang Engineering Geology 242 (2018) 150–159

$\nu_{\rm n}, \nu_{\rm t}$	Normal and Tangential components of velocity on
	sliding surface
W_{γ}	External work rate due to soil weight
Z	Distance from a generic point within slope to water
	table level
z_{3D} , z_{insert}	Vertical distance from a generic point on sliding
	surface to water table level for 3D portion and
	inserted portion
z_0	Vertical distance from water table to slope toe

1. Introduction

Slope stability assessment is one of the most classic and long-standing subjects in the geotechnical literature, which has historically been performed using 2D plane-strain failure mechanisms (Chen, 1975; Griffiths and Lu, 2005; Zhu et al., 2011; Li et al., 2014; Zheng et al., 2014; Qin and Chian, 2018). However, slope failures usually show an obvious 3D feature in engineering, which suggests that the plane-strain failure mechanisms cannot truly reflect the collapse of slopes. To derive a more realistic solution, it is of great practical significance to conduct an analysis for the stability of 3D slopes. In this regard, several approaches have been developed and can be grouped into three main categories: (i) traditional limit equilibrium methods; (ii) numerical simulations; and (iii) limit analysis.

The limit equilibrium methods still play the most popular role in the stability estimation of 3D slopes, and they are usually a direct extension of various 2D methods (Hungr et al., 1989; Wei et al., 2009; Zhou and Cheng, 2013). Therefore, most of these methods contain the same assumptions about the distribution of stresses and failure surfaces as the 2D methods, which may not be satisfied under 3D conditions. Moreover, the results obtained by limit equilibrium are neither upper bounds nor lower bounds. Numerical approaches including the finite element method and the discrete element method have also gained significant attention (Ugai and Leshchinsky, 1995; Griffiths and Marquez, 2007; Liu et al., 2017). In addition, several more advanced numerical methods have been developed, such as dual-horizon peridynamics (Ren et al., 2016, 2017), cracking-particle method (Rabczuk and Belytschko, 2004; Rabczuk et al., 2010), efficient remeshing techniques (Areias et al., 2013; Areias and Rabczuk, 2017), screened-Poisson equation models (Areias et al., 2016) and specific designed softening elements (Areias et al., 2014). These advanced methods all have the potential to be extended to analyze the stability of 3D slopes. However, the level of expertise required to perform such advanced simulations and the difficulties in modeling and result validation have prevented their widespread application. Furthermore, the simulations of complex parameters, e.g., soil suction in this study, have also posed major challenges, particularly under 3D conditions.

Alternatively, the kinematic limit analysis method has also been extensively applied to the stability analysis of 3D slopes (Michalowski, 1989; Michalowski and Drescher, 2009; Xu and Yang, 2018). Its main advantage lies in its ability to account for different complex factors that affect slope stability. When the kinematic approach is used in the 3D cases, the most important but most difficult task is to construct an admissible failure mechanism. Until now, only a limited number of 3D failure mechanisms have been proposed. Michalowski (1989) constructed a multi-block failure mechanism to assess the stability of 3D slopes. Gens et al. (1988) developed a cylindrical and spherical mechanism for the stability of 3D slopes in purely cohesive soils. More recently, the horn failure mechanism pioneered by Michalowski and Drescher (2009) has been widely used to study the effect of different factors on the slope stability. For example, Gao et al. (2015) employed the 3D horn mechanism to analyze the effect of soil strength nonlinearity on the stability of slopes. Xu and Yang (2018) presented a solution to the seismic stability of 3D reinforced slopes in nonhomogeneous and anisotropic soils on the basis of the horn mechanism.

Park and Michalowski (2017) extended the horn failure mechanism for the stability assessment of 3D slopes in bonded geomaterials with tension cut-off in the yield surface. Compared with the other two failure mechanisms, the horn failure mechanism is more critical and more applicable. This occurs because the results obtained from the 3D horn mechanism are more critical than those from the multi-block mechanism and because the 3D horn failure mechanism will degenerate to the cylindrical and spherical mechanism when the analyzed soil is purely cohesive.

The aforementioned works were primarily limited to slopes in completely dry or completely saturated soils. However, soils are usually unsaturated. Many precipitation-induced slope failures have been reported to occur in unsaturated soils (Lu et al., 2013; Sorbino and Nicotera, 2013). Therefore, an appropriate approach that explicitly considers the effect of matric suction in slope engineering is required.

Due to the existence of matric suction, there exists significant difference in the shear strength behavior between unsaturated soils and dry or saturated soils. Therefore, the stability analysis of unsaturated slopes cannot be realized unless a more general yield criterion for unsaturated soils is established. In this respect, Fredlund et al. (1978) proposed a modification to the linear Mohr-Coulomb yield criterion to account for the suction effect, where the increase in unsaturated shear strength is assumed to be linear along with the soil suction by assuming a constant suction angle φ^b (e.g., $\varphi^b=15^\circ$). This modified criterion has been applied in some studies to discuss the impact of soil suction on the stability of slopes (Gavin and Xue, 2010). However, it was later well recognized that the suction angle φ^b is not a constant and that the relationship between the shear strength of unsaturated soils and matric suction has a highly nonlinear form (Fredlund et al., 1996; Vahedifard et al., 2016). Furthermore, most of the aforementioned studies considered the soil suction as an independent stress variable and assumed the suction to be uniform or linear along the depth. In reality, the soil suction is highly nonlinearly distributed along the vertical axis. The assumption of uniform or linear distributions of soil suction will cause inaccurate estimates of unsaturated shear strength and, ultimately, is inappropriate for assessing the stability of an unsaturated slope.

Previous studies also brought up a discussion about the use of soil suction as a stress variable. It has been argued that the soil suction is not a stress variable but is highly dependent on other parameters (Lu, 2008; Vahedifard et al., 2015, 2016). Reasonable success has been achieved in estimating the suction stress of soils under unsaturated steady flow conditions (Griffiths and Lu, 2005; Lu and Godt, 2008), in which four new parameters are involved, one for the flow conditions and the others for the soil types. Thus, several studies have been performed to investigate how the slope stability is affected by the matric suction with unsaturated flow effect. For example, Griffiths and Lu (2005) used the elasto-plastic finite element method to analyze the unsaturated slope stability. Lu and Godt (2008) established a generalized approach to estimate the stability of infinite unsaturated slopes. Vahedifard et al. (2016) presented a solution to the stability of unsaturated slopes by using the principle of moment equilibrium. These investigations considered the variation of saturation caused by the flow effect, leading to more accurate estimates of the slope stability under unsaturated con-

Notwithstanding the significance of the contributions mentioned above, the stability of 3D unsaturated slopes is an interesting topic that has not yet been satisfactorily studied. The principal aim of this study, therefore, is to present a more general approach for estimating the stability of 3D slopes subjected to vertical steady unsaturated seepage effect. To do this, a closed-form representation about the shear strength of unsaturated soils is incorporated into the kinematic limit analysis method. The widely used 3D horn failure mechanism of Michalowski and Drescher (2009) is adopted to calculate the internal energy dissipation rate and external work rate. The cohesion required for bringing a slope to the limit failure state is calculated and listed in the form of a stability number. A powerful routine is used to search for the maximum

Download English Version:

https://daneshyari.com/en/article/8915831

Download Persian Version:

https://daneshyari.com/article/8915831

<u>Daneshyari.com</u>